SELECTIVE DOLOMITIZATION BY SYNTAXIAL OVERGROWTH AROUND DETRITAL DOLOMITE NUCLEI: A CASE FROM THE JURASSIC OF THE LIGURIAN BRIANCONNAIS (LIGURIAN ALPS)

Published version:

DOI:10.2110/jsr.2014.2

SELECTIVE DOLOMITIZATION BY SYNTAXIAL OVERGROWTH AROUND DETRITAL DOLOMITE NUCLEI: A CASE FROM THE JURASSIC OF THE LIGURIAN BRIANÇONNAIS (LIGURIAN ALPS)

LUCA MARTIR E*[1], CARLO BERTOK[1], ANNA D'ATRI[1], ELENA PEROTTI[1], FABRIZIO PIANA[2]

** luca.martire@unito.it*

[1] *Dipartimento di Scienze della Terra, University of Torino, via Valperga Caluso 35, 10125 Torino, Italy*

[2] *Istituto di Geoscienze e Georisorse, Torino section, CNR, via Valperga Caluso 35, 10125 Torino, Italy*

Running title: SYNTAXIAL OVERGROWTH OF DETRITAL DOLOMITE

Key words: Detrital dolomite, syntaxial overgrowth, Jurassic, Ligurian Briançonnais, French-Italian Ligurian Alps.

ABSTRACT

Dolomite crystals, occurring in Middle Jurassic dolostones and dolomitic limestones of the Ligurian Briançonnais Domain (French-Italian Ligurian Alps), show irregular, complex zoning evidenced by cathodoluminescence (CL) and backscattered electron imaging. Comparable zoning patterns from other study areas have been attributed alternatively to recrystallization or dissolution-precipitation processes. However, none of these mechanisms can account for the range of observations from the Ligurian Briançonnais Domain, which include: 1) the presence of multiple core types, each with different CL characteristics; 2) marked compositional differences between cores and surrounding rims (ferroan vs. nonferroan, Mg/Ca ratio); 3) a marked shape difference between cores, with irregular outlines, and rims which progressively approach a well-developed rhombohedral habit. These features are most reasonably interpreted as dolomitic rims that formed as syntaxial overgrowths around detrital dolomite nuclei, which in turn originated from erosion of underlying Triassic rocks and triggered selective replacement of fine-grained calcareous sediment. Failure to recognize the exact nature of this type of dolomite crystal may lead to overestimating the degree of dolomitization and to overlooking possible detrital inputs in a basin otherwise supplied with pure allochemical sediments, with consequent loss of information on the tectonosedimentary evolution.

INTRODUCTION

The modes and environments of dolomitization of carbonate sediments are still an open and controversial problem in earth sciences. This ambiguity is due mainly to the fact that an actualistic approach seems to be largely inadequate, as the great abundance of dolomite in the geological past is at odds with its fairly rare occurrence in Holocene sediments (e.g., Hardie, 1987; Machel, 2004; Meister et al., 2013). The study of zoning in dolomite crystals provided important insights into dolomite formation mechanisms, showing that a number of processes, well known in limestone diagenesis, including recrystallization, dissolution, and void-filling cement precipitation, may be common in dolostones too (e.g., Harris and Meyers, 1987; Cander et al., 1988; Gregg and Shelton, 1990; Gregg et al., 1993; Machel, 1997; Reinhold, 1998; Jones, 2005, 2007; Ehrenberg et al., 2006; Choquette and Hiatt, 2008). Zoning refers to spatial differences of composition within a crystal (Reeder, 1991) and, leaving aside sectoral zoning, may display a great variety of patterns: crystals may be alternatively homogeneous (i.e., nonzoned), concentrically zoned with zone boundaries parallel to crystal faces, concentrically zoned with irregular zone boundaries, or "chaotically zoned" (i.e., displaying complex patchy distribution of compositionally different portions). Zoning reflects changing conditions during crystal growth, from rapid growth in stable conditions, to steady state growth under slightly changing chemical parameters, to more complex evolution of diagenetic processes involving discontinuous growth, dissolution, and recrystallization. Cathodoluminescence, because of its high sensitivity to minor geochemical changes in the diagenetic environment (e.g., activator and quencher concentration, Eh and pH, ion activity, growth rates; Machel and Burton, 1991; Machel, 2000), is a useful technique to highlight zoning. Cathodoluminescence moreover allows identification of the most suitable portions of the crystals for carrying out further analyses aimed at characterizing quantitatively the geochemical features of the different zones (e.g., Mg/Ca ratios, Fe and Mn content, $\delta^{18}O$ and $\delta\ ^{13}C$).

Studies on dolomitization, performed with this kind of petrographically controlled approach, led recently to reinterpretations of previously described case histories. For example, Choquette and Hiatt (2008) provided a new possible explanation of common fabrics in sucrosic dolostones such as the so-called CCCR (cloudy-centered clear-rimmed dolomite: Murray, 1964; Sibley, 1982): they showed that the cloudy cores consist of replacive dolomite, whereas clear rims consist of a dolomite cement filling secondary pores generated by limestone dissolution. On the other hand, dissolution of dolomite crystals followed by centripetal dolomite cementation in the resulting hollows (inside-out dolomite: Jones 2007) has been proposed as an alternative hypothesis for explaining complex zoning patterns that other authors related to recrystallization (Harris and Meyers, 1987; Cander et al., 1988; Reinhold, 1998).

Complex zoning patterns have been recognized in dolomite contained in Middle Jurassic dolomitic limestones of the Ligurian Briançonnais (Ligurian Alps, NW Italy) (Fig.1). Stratigraphic, sedimentologic, petrographic, and geochemical evidence collectively indicate that none of the above-mentioned processes can account for the observed pattern. This contribution does not discuss all aspects of the dolomitization of the Jurassic limestones of the Ligurian Briançonnais; it is rather focused on the description and interpretation of particular zoning patterns that may be of general interest for researchers working on variably dolomitized strata. The purpose of this study is to explore the possible importance of a different mechanism, a selective limestone replacement as syntaxial overgrowths of dolomite around detrital grains.. The identification of this kind of dolomite in fact documents the presence of terrigenous grains which otherwise could be unrecognized in apparently pure allochemical rocks. This in turn may provide solid evidence of syndepositional faulting that resulted in exhumation and erosion of older dolomitic formations. The diagenetic evolution is also simplified as it changes from a complex sequence of events (dissolution, reprecipitation, or recrystallization) to a single phase of dolomite growth around detrital cores. Because it provides new insights, the syntaxially overgrown detrital dolomite (SODD) hypothesis may be applicable to understanding other dolomites in the geologic record that do not find satisfactory explanations in the existing models.

GEOLOGICAL SETTING

The Briançonnais Domain is one of the first-order tectonic units of the Alpine orogen (Fig. 1). It crops out from the Swiss Alps to the Ligurian Alps, where it is labelled “Ligurian Briançonnais.” In the frame of Alpine paleogeography, the Briançonnais has been interpreted as a highstanding block, individuated during Late Triassic-Early Jurassic rifting, along the distal portion of the European continental margin, bordering the western Tethys basin (Vanossi et al., 1984; Lemoine et al., 1986; Lemoine and Trümpy, 1987; Lanteaume et al., 1990; Mohn et al., 2010). Alpine deformation and metamorphism of the Briançonnais Domain generally decrease westward, i.e., from the internal to the external parts. The study area is located in the exterior part (External Ligurian Briançonnais)(Fig. 1), where deformation generated pervasive tectonic foliations confined to marly and clayey intervals of the succession (Piana et al., 2009). Consequently, primary stratigraphic features, such as depositional geometries, facies, and microfacies, are largely preserved in carbonate sedimentary units.

The Ligurian Briançonnais consists of Permian volcanic and volcanosedimentary rocks overlain by a Mesozoic-Cenozoic sedimentary succession that includes (Vanossi et al., 1984; Lanteaume et al., 1990; Bertok et al., 2011) (Fig. 2): Upper Permian (?)-Lower Triassic conglomerates and littoral cross-bedded quartz arenite (Quarziti di Ponte di Nava, QPN: over 100 m) overlain by Lower Triassic lagoonal mudrock 10-15 m thick (Peliti di Case Valmarenca, PCV); Middle Triassic peritidal dolostone and dolomitic limestone (Dolomie di San Pietro dei Monti, DSPM: about 300 m), bounded at the top by a Late Triassic to Middle Jurassic stratigraphic hiatus caused by subaerial exposure; Middle Jurassic inner-shelf limestone and dolomitic limestone (Calcari di Rio di Nava, CRN: 20-90 m); Upper Jurassic pelagic limestone, locally showing a Rosso Ammonitico facies (Calcari di Val Tanarello, CVT: 10-60 m), bounded at the top by an important stratigraphic discontinuity; Upper Cretaceous hemipelagic sediment (Formazione di Upega, FU: about 100 m); Middle Eocene nummulite-rich limestone (Calcari della Madonna dei Cancelli, CMC: about 30 m), overlying another unconformity and followed by hemipelagic and turbiditic sediment (Flysch Noir, FN). Clear evidence of Middle Jurassic to Cretaceous post-rifting, syndepositional tectonic activity, with extensional and transcurrent components, has recently been documented in the study area (Bertok et al., 2011, 2012).

MATERIALS AND METHODS

This study is focused on the dolomite occurring in the Middle Jurassic CRN inner shelf carbonates that range from almost pure dolostone to slightly dolomitic micritic limestone. Middle Triassic dolomites have not been studied in detail, but only for purposes of comparison. Several sections have been studied and sampled, spread over an area of about 10 km^2 (for location and stratigraphy refer to Bertok et al., 2011). Petrographic studies of polished thin sections prepared from about 30 specimens were carried out by plane-light, cross-polarized-light, and cathodoluminescence (CL) microscopy, performed with CITL 8200 mk3 equipment (working conditions: approximately 17 kV and 400 μA) to identify zoning in crystals. Backscattered electron imaging (BSE) of polished thin sections was also carried out with a Cambridge Stereoscan 360 SEM instrument, which allowed differentiation between calcite and dolomite on a microscopic scale, and, together with microprobe analyses, provided an opportunity to relate CL colors and intensities to intracrystal compositional changes. Twenty seven *in situ* quantitative microprobe analyses on dolomite crystals were performed with an EDS Energy 200 and a Pentafet detector (Oxford Instruments) associated with the SEM. The operating conditions were: 15 kV accelerating voltage, around 1 nA of probe current, and 50 seconds counting time. SEM-EDS quantitative data (spot size = 2 μm) were acquired and processed using the Microanalysis Suite Issue 12, INCA Suite version 4.01; SPI natural mineral standards were used to calibrate the raw data; the RoPhiZeta correction (Pouchou and Pichoir, 1988) was applied. Analytical statistical errors Σ on atomic weight % are 0.08 for Mg and Fe and 0.13 for Ca.

DOLOMITE: OCCURRENCE AND FEATURES

In the Mesozoic succession of the External Ligurian Briançonnais Domain, dolomite occurs in the Middle Triassic DSPM and the Middle Jurassic CRN lithostratigraphic units. The DSPM consists mainly of pure dolostones that exhibit different facies (mainly dolomicrite, massive or thinly laminated, characterized by fenestrae or gypsum pseudomorphs, and subordinate peloidal grainstone with flaser bedding and breccias) all reflective of a peritidal depositional environment. These rocks mainly consist of very finely to finely crystalline dolomites (less than 10 μm to tens of μm) resulting from a nondestructive replacement of micritic sediments. Very coarsely crystalline dolomite (up to some millimeters) also occurs as a cement filling shrinkage pores and vugs.

Replacive dolomite displays CL colors ranging from nonluminescent (NL), to moderate to dull red and greenish, depending on the beds (Fig. 3); void-filling dolomite cements displays moderate- to bright-red colors. EDS analyses show that replacive dolomite consists of systematically nonferroan and nearly stoichiometric dolomite (Ca:Mg molar ratio ranging from 1.0:1.0 to 1.05:0.95; low-Ca calcian dolomite, LCD, of Jones and Luth, 2002)(N=4). Al_2O_3, SiO_2, and K_2O have also been detected (total percentage around 2-3%) which point to the presence of a minor clay fraction.

Middle Jurassic CRN limestones show a variable degree of dolomitization that generally decreases from the stratigraphic bottom to the top and that ranges from complete (at the very base in one section, lowermost 50 cm) to only minor (less than about 5% dolomite in the uppermost part). The most widespread limestone lithofacies consist of mudstone to wackestone with sparse crinoid fragments and benthic foraminifera. Millimeter- to centimeter-size angular to rounded clasts of dolostone occur at the very base as a transgressive lag over the Upper Triassic – Lower Jurassic subaerial discontinuity surface. Single dolomite crystals, up to 200 μm in size, with a pitted, irregular outline locally occur as nuclei of coated grains (ooids, microoncoids) in the matrix of such transgressive conglomerate (Fig. 4). In some sections, angular to rounded, millimeter- to centimeter-size clasts of dolostone also are present in the lower part of the Middle Jurassic limestone, in centimeters- to decimeters-thick beds of matrix- to clast-supported breccia (Fig. 5). The common occurrence of shrinkage pores in dolostone clasts documents their provenance from the underlying Middle Triassic DSPM. Dolomite in pure dolostone at the very base of the CRN occurs mainly as subhedral to euhedral crystals with planar faces (Fig. 3); crystal size is fairly homogeneous, at approximately 100 μm. CL observations reveal that most dolomite crystals contain irregularly shaped cores, mainly NL but also showing dull red and greenish luminescence. The cores are surrounded by a thin bright orange rim. Scattered dull-blue-luminescing quartz grains with the same size as dolomite crystals can also be recognized (Fig. 3)

Dolomite in CRN dolomitic limestone occurs as euhedral to subhedral crystals of variable size (15 to 150 μm). They have irregularly shaped cores, 10 to 100 μm in size. Core edges are generally highly irregular, angular, and with embayments, whereas planar edges and subrounded shapes are uncommon (Figs. 6, 7, 8). Cores show the same CL features as those of the underlying pure dolostone (mainly NL but also dull red and greenish) but are surrounded by more developed and complexly zoned rims. The most common pattern is represented by an inner bright-orange zone, directly surrounding the core, followed outward by a middle moderate-orange zone and by an outer NL zone (Figs. 6, 7, 8). Local deviations from this common pattern include additional discontinuous, bright-orange hairline zones. The markedly different colors enable clear observation of the geometry of the interfaces between the different zones. Whereas cores display highly irregular edges, with smooth to angular to very jagged outlines, outer zones tend to increasingly approach the rhombic habit, so that each zone is thicker where the core edge was farther from the rhomb faces. A quasi-perfect parallelism between zone interfaces and euhedral outer faces of the crystal usually is reached only by the moderate-orange-NL boundary. The small size of the cores and zoned rims commonly hinders accurate EDS analyses. However, where possible, analyses reveal that NL nuclei and orange CL zones are nonferroan, whereas the NL outer zone is commonly slightly ferroan (0.7 – 2.0 mole % $FeCO_3$). Moreover, the Ca:Mg ratio varies from 1.05:0.95 to 1.07:0.93 (average 1.06:0.94) in the cores (low-Ca calcian dolomite, LCD, of Jones and Luth, 2002) (N=2) and from 1.08:0.92 to 1.19:0.81 in the rims (average 1.13:0.87, i.e., mostly high-Ca calcian dolomite, HCD, of Jones and Luth, 2002) (N=11) (Fig. 9). BSE imaging also reveals zoning with crystals exhibiting homogeneous, darker cores and lighter rims. Outer rims also are characterized by brighter micrometer-size irregular spots composed of calcite (Fig. 10).

Polycrystalline dolomite lithoclasts are also present; they are up to some hundred micrometers in size and consist of decimicrometer-size crystals. They show a homogeneous cathodoluminescence, which may be greenish, dull red, or NL, and are not surrounded by zoned rims (Fig. 11). The Ca:Mg ratios (from 1.03:0.97 to 1.04:0.96) (N=2), nonferroan composition, CL features, and presence of SiO_2 and Al_2O_3 allow comparison of these polycrystalline lithoclasts with Triassic dolostone.

Dolomite also occurs as a coarsely crystalline mosaic, infilling a network of mainly subvertical veins, up to 2 mm wide, which are locally developed. Veins crosscut the Middle Triassic DSPM -Middle Jurassic CRN unit boundary and taper out, within some decimeters higher up in the section, where the Jurassic strata display a gradual transition from fully dolomitized, at the base, to partially dolomitized. A marked zoning of dolomite filling the veins is immediately apparent from CL observation, with the following sequence (from inner to outer parts): I) NL, II) bright orange, III) moderate orange, and IV) NL (Fig. 12). The two NL zones are ferroan (1.7 – 3% $FeCO_3$) (N=8) whereas the orange luminescing zones are nonferroan as is also well evidenced by BSE images (Fig. 12).

DISCUSSION

The features of dolomite observed in the Middle Jurassic carbonate rocks of the External Ligurian Briançonnais Domain can be summarized as follows:

1) in the lower part of the CRN, lithoclastic breccia or conglomerate with dolostone clasts are interbedded with micritic limestone. These beds have been interpreted as the result of storm-induced currents transporting offshore clasts eroded from rocky coasts locally developed on Middle Triassic, subaerially exposed, dolostone (Bertok et al., 2011);

2) monocrystalline dolomite grains occur as nuclei of coated grains in the lower part of the CRN;

3) dolomite crystals are present throughout the CRN but are particularly abundant in the lower part, where they are associated with quartz grains of comparable size and polycrystalline dolomite lithoclasts up to some hundreds of micrometers in size;

4) dolomite crystals are zoned under CL and display homogeneous cores and zoned rims; cores are irregularly shaped, whereas rims show increasingly better developed rhombohedral crystal faces progressing outwards;

5) cores of dolomite crystals, occurring side by side in the same thin section, show a conspicuous variability in CL features (NL, dull red, greenish);

6) independently of the size and CL color of the core, rims show the same succession of CL zones;

7) vein-filling sparry dolomite mosaics show four CL zones (NL, bright orange, moderate orange, NL), three of which (bright orange, moderate orange, NL) correlate with rims of rhombs;

8) polycrystalline dolomite lithoclasts are not surrounded by zoned rims;

9) compositional features (CL, BSE, Ca:Mg ratios, ferroan vs. nonferroan, presence or absence of SiO_2 and Al_2O_3) show that cores are different from rims but indistinguishable from Middle Triassic dolostones and polycrystalline clasts occurring in the lower part of the CRN.

Points 1 and 2 demonstrate that a dismantlement of Middle Triassic dolostone was taking place in the Middle Jurassic during deposition of CRN. Finely crystalline dolostone gave rise to polycrystalline lithoclasts of a size ranging from fine sand to pebbles. More coarsely crystalline dolostone or fenestral pore-filling dolomite cements, instead, could weather out to monocrystalline grains that were transported to a shallow marine environment where they acted as nuclei for coated grains. Point 3 confirms that terrigenous grains were shed into the CRN basin and documents that denudation and exposure affected also the Lower Triassic quartzarenites (QPN). Points 4, 5, and 6 document that the cores of dolomite crystals are primary elements of the Middle Jurassic sediment whereas rims result from a common diagenetic evolution recorded by all dolomite rhombs. Point 7, together with Point 4, proves that rims and vein-filling dolomite are coeval and cogenetical and that rims grew outwards starting from the outer edges of cores. However, it is important to note that the innermost zone of vein dolomite, which is NL, ferroan, and thus brighter in BSE, has no counterpart in the rhombs and cannot be related to the NL cores (Figs. 9, 12, 13). Point 8 shows that monocrystalline cores were necessary to trigger dolomite precipitation, which, conversely, did not take place around fine-grained, polycrystalline lithoclasts. Point 9, together with Points 1, 2, 3, and

5, indicates that both polycrystalline clasts and dolomite crystal cores could be fragments of Middle Triassic DSPM dolostone reworked into the Middle Jurassic CRN.

Detrital dolomite is not a novelty in the geological literature. It has been reported in a wide array of stratigraphic and paleoenvironmental settings. The most obvious occurrence is in terrigenous sediments whose source areas include carbonate successions (e.g., Ordovician non marine sandstones, Texas: Amsbury 1962; Cretaceous coastal plain sandstones, Utah: Taylor et al 2000, 2004; Cretaceous glauconitic sandstones, Alberta: Young and Doig, 1986; Miocene turbidites, Italian Apennines: Gandolfi et al., 1983). Dolomite grains found in mixed sediments deposited in cool-water platforms (Plio-Pleistocene, Australia: Bone et al 1992, James and Bone 2007; Miocene, Menorca: Freeman et al., 1983) have a comparable origin. Carbonate successions may include limited lithosomes of detrital dolomites interpreted as infillings of karstic cavities (e.g., Devonian, Canada: Morrow et al 1986; Ordovician, Virginia: Mussman and Read, 1986). Recent deep-sea sediment also contains detrital-dolomite-rich beds that have been correlated to climatic changes in turn affecting aridity, and thus eolian transport (e.g., Cullen et al 2000), or ice sheet dynamics (Andrews and Tedesco, 1992; Knies et al., 1999; Ji et al 2009). Detrital dolomite was also reported in ancient marine limestones and related to eolian transport of penecontemporaneous dolomite from tidal flats or from the erosion of older carbonate rocks (Devonian, New York: Lindholm, 1969; lower Palaeozoic, Newfoundland: Coniglio and James, 1988). The most impressive report of a sedimentary body consisting almost entirely of terrigenous dolomite is the Pennsylvanian Atoka Dolomite, several hundred meters thick, resulting from deposition in a fan-delta environment of sediments eroded from Ordovician dolomites (Lyday, 1985). Many papers, moreover, highlight the important role of detrital dolomite grains as nuclei for growth of authigenic dolomite (Lindholm, 1969; Freeman et al., 1983; Bone et al 1992).

On the basis of the data and considerations reported above, it appears that the dolomite in the Middle Jurassic CRN resulted from a process of replacement of calcareous sediment occurring as selective overgrowth of authigenic syntaxial dolomite around silt- to sand-size, irregular, monocrystalline grains of detrital dolomite (SODD: syntaxially overgrown detrital dolomite) (Fig. 13). These grains consist of clasts of reworked Middle Triassic DSPM dolostone showing non-, red or greenish luminescence, depending on the stratigraphic level from where clasts were sourced. Silt- to sand-size dolomitic detritus came from the same areas as the breccia-bed clasts, but it was finer grained, scattered within Middle Jurassic sediment, and progressively decreasing in quantity going up-section. The uppermost part of the Middle Triassic dolostones between the Late Triassic and the Early Jurassic underwent a prolonged emersion that locally generated karstic cavities with terra rossa infillings (e.g., Faure and Megard-Galli, 1988; Decarlis and Lualdi, 2008). The Middle Jurassic sea consequently transgressed over rocky coasts made up of dolostones that had never been deeply buried and thus were likely characterized by a typical intercrystalline porosity, possibly enhanced by emersion-related dissolution. The mechanical action of shallow marine processes (waves, storms etc.) led to the surficial disaggregation of these rocks, producing both coarse polycrystalline clasts and finer-grained debris of single dolomite crystals whose external shape may reflect the original euhedral outline, mechanical breakage, or chemical corrosion. The limited degree of transport, probably mainly due to short-lived storm episodes (cf. Bertok et al., 2011), accounts for the very low roundness of detrital cores.

The occurrence of detrital dolomite throughout the whole Middle Jurassic CRN, some tens of meters thick, shows that the reworking of the Middle Triassic dolomites was not limited to the earliest phase of transgression. This in turn implies that the Middle Jurassic transgression did not take place over the top of a flat platform but affected a rugged topography that allowed the survival of coastal or even emergent portions of the former Triassic platform. This is also confirmed by the direct superposition of Upper Jurassic limestones over Middle Triassic dolostones in adjacent areas (Vanossi, 1965) and by independent stratigraphic and sedimentologic evidence pointing to faulting processes before and during CRN deposition (Bertok et al., 2011).

Detrital dolomite grains, now corresponding to the cores of zoned dolomite rhombs, acted as nucleation sites for authigenic dolomite overgrowth. The widespread micrometer-size calcite inclusions, very well imaged by BSE (Fig. 10) in the rims but absent in the cores, likely consist of undolomitized portions of the original calcareous sediment, possibly corresponding to very fine-grained fragments of skeletal grains.

At the base of the CRN succession, where detrital dolomite grains were closely packed, pure dolostone were formed where the entire sequence of authigenic dolomite zones could not be recorded; the latter were thicker and well developed in partially dolomitized mud-supported facies with widely spaced dolomite grains. Each younger zone of authigenic dolomite contributed to improve the outer crystal, habit increasingly approaching the rhombohedron that is almost perfectly developed with the last, NL growth stage (Phases 3 and 4 in Fig. 13). This preferential growth towards the rhombohedron edges, and in particular the acute ones, is reminiscent of the syntaxial cements around echinoderm plates that grow at faster rates perpendicular to the plate edge i.e., along the *c* axis (e.g., Evamy and Shearman, 1965; Walkden and Berry, 1984).

The data also permit some thermodynamic inferences about the chemistry of the diagenetic fluids flowing through these sediments (cf. Machel, 2004). The occurrence of a first NL ferroan dolomite generation only within veins could be explained as the result of an early cementation phase by fluids that were supersaturated with respect to dolomite but not undersaturated with respect to calcite (phase 2 in Fig. 13). They therefore allowed precipitation of dolomite in open fractures, but not replacement of calcareous sediments. Subsequently, fluids became undersaturated with respect to calcite and only slightly supersaturated with respect to dolomite, so that dolomite could precipitate by syntaxial overgrowth around a dolomite substrate. This substrate was provided by detrital grains in sediments and by the first-stage dolomite crystals in veins.

Dolomite crystals with comparable zoning patterns have been commonly reported in the literature. Basically, interpretations call upon recrystallization during burial (e.g., Harris and Meyers, 1987; Cander et al., 1988; Reinhold, 1998), dissolution taking place during crystal growth (e.g., Gregg et al., 1993), or intracrystalline dissolution of the core and precipitation of dolomite cement in the resulting pore (inside-out dolomite: Jones, 2005, 2007).

In the case studied here, dolomite nuclei show a variety of CL emissions (NL, dull red, greenish) and are surrounded by rims with the same dolomite CL stratigraphy (bright orange, moderate orange, NL from the core outwards). The NL dolomite of the outer rim is a ferroan HCD whereas that of the NL nuclei is a non ferroan LCD, i.e. ,they are compositionally very distinct. Moreover, the variability in CL of the cores indicates that they cannot be interpreted as cements filling intracrystalline voids formed by selective dissolution, unless several phases of very patchy precipitation of dolomite cements with different CL are taken into account. Because such complex process seems very unlikely and no evidence of dissolution is recognizable in the dolomite lithoclasts, the inside-out model (Jones, 2007) cannot be applied to our case. Furthermore, the good correlation of the CL zones bright orange, moderate orange, NL in core-surrounding rims from rhombs to vein-filling dolomite definitely proves that rims grew outwards and confutes the inside-out hypothesis that conversely would involve an inward growth of dolomite cement in a dissolution cavity.

The absence of dissolution features, both in dolomite lithoclasts and in vein-filling dolomite where CL zones are separated by perfectly planar boundaries (Fig. 10), is a valid argument to exclude the possibility of an interruption in crystal growth, associated with some dissolution, and followed by renewed precipitation over a pitted surface, as proposed by Gregg et al. (1993). The shape of the surfaces separating rim dolomite zones (bright orange, moderate orange, NL), roughly subparallel to core edges and developing increasingly euhedral habits progressing outwards, further supports this conclusion and allows to rule out also the hypothesis of recrystallization (Harris and Meyers, 1987; Cander et al., 1988; Reinhold, 1998). The latter would have produced a more chaotic, patchy, luminescence.

The recognition that zoned dolomite crystals may be due to diagenetic overgrowth around inherited, detrital grains goes beyond the mere petrographic aspect and involves wider geological implications. The most relevant conclusion of general interest of this study is that dolomite crystals showing the features here described are *per se* evidence of the presence of detrital grains of extrabasinal origin. This may be trivial in terrigenous or mixed sediments but is of utmost importance in presumably pure allochemical rocks, such as dolostones or dolomitic limestones, in which the growth of diagenetic dolomite masks the presence of a pristine inherited clastic component. If dolomitic formations occur stratigraphically below the SODD-bearing rocks, as in the present case study, some kind of faulting leading to superficial exposure and erosion of previously buried rocks is documented. If instead there is no dolomitic body in the local stratigraphy, the source of the detrital dolomite cores should be searched in allochthonous terranes. In both cases recognition of SODD may provide an additional or even unique clue to syndepositional tectonics.

The second conclusion refers to the diagenetic evolution. The hypothesis here proposed of syntaxially overgrown detrital dolomite implies only a single phase of dolomite precipitation whereas other models, calling upon dissolution, reprecipitation, or recrystallization, involve a more complex diagenetic evolution with obvious implications over patterns of fluid flow through sedimentary-basin infills.

Moreover, the SODD hypothesis imposes a re-evaluation of the actual degree of dolomitization in dolomitic limestones and dolostones since only the overgrowths could be due to calcite replacement. In principle, some dolostones could consist mostly of detrital dolomite, with authigenic dolomite representing only a minor part of the whole rock volume, as it has indeed been reported already in literature (e.g., Lyday, 1985).

Lastly, this study shows that dolomitization may be very selective and it may take place only around detrital dolomite grains. It is worth highlighting that in the absence of such clasts no dolomitization takes place and the flow of potentially dolomitizing fluids leaves no evidence.

On the basis of what is discussed above, the main difference of this paper with respect to the one by Choquette and Hiatt (2008), which treats a similar topic, concerns the implications. The major conclusion by Choquette and Hiatt (2008) is that a significant part of sucrosic dolostones results from free-space cementation and not replacement. The detrital origin of dolomite cores was just hypothesized, as a possible alternative to an authigenic origin, due to their small size, substantially of a few micrometers, making them not easily visible in thin section. In the case described in the present paper, dolomite cores commonly reach a fine-sand grain size, give rise to a complex zoning of dolomite rhombs which is perfectly recognizable in thin section, and represent a significant portion of the whole dolomite volume. Therefore, the focus here lies in the proposal of a further model for explaining irregularly zoned dolomite rhombs that adds to the existing ones involving dissolution during growth, dissolution after full rhomb growth, and recementation, or recrystallization.

CONCLUSIONS

- Stratigraphic, sedimentologic, petrographic, and geochemical evidence from the Middle Jurassic CRN dolomitic limestone and dolostone of the Ligurian Briançonnais Domain (French-Italian Ligurian Alps) document that irregularly zoned dolomite crystals consist of two distinct domains: an irregularly shaped core of detrital origin and an authigenic rim related to postdepositional diagenesis.

- Dolomite cores originated as the monocrystalline component of a detrital input that included also polycrystalline clasts ranging in size from fine sand to pebbles. They were eroded from exposed portions of Middle Triassic dolostone and delivered to the shallow marine CRN basin.

- Dolomitization of Middle Jurassic CRN limestone was very selective and proceeded only around the irregular fragments of detrital dolomite grains, giving rise to syntaxial overgrowths.

- Dolomite overgrowth around detrital cores provides another possible explanation for irregularly zoned dolomite rhombs in addition to dissolution, reprecipitation, or recrystallization. In spite of a great deal of research on dolomitization, such a process has not been kept in due consideration so far. Although more than forty years have passed, a statement by Lindholm (1969) seems to be still a very living issue: “The role of detrital dolomite in carbonate sedimentation and diagenesis warrants attention in future works." Actually not all dolomite in a dolomite-bearing carbonate rock may be due to dolomitization.

- The recognition of SODD documents the presence of terrigenous grains which otherwise could be unrecognized in apparently pure allochemical rocks. It may also provide indirect evidence of syndepositional tectonics resulting in fault-related exhumation of previously buried formations or even the emplacement of allochthonous units.

AKNOWLEDGMENTS

We are indebted to Editor Gene Rankey, Associate Editor Leslie Melim, and the two referees Brian Jones and Sean Loyd, for the valuable comments and suggestions that greatly improved the manuscript. Many thanks to Marco Beltrando (Torino) for the great (and quick!) work on the English language. The CNR-IGG (Torino section) is gratefully acknowledged for the financial support in researches on Ligurian Alps geology.

REFERENCES

AMSBURY, D.L., 1962, Detrital dolomite in Central Texas: Journal of Sedimentary Petrology, v. 32, p. 5−14.

ANDREWS, J.T., AND TEDESCO, K., 1992, Detrital carbonate-rich sediments, northwestern Labrador Sea: implications for ice-sheet dynamics and iceberg rafting (Heinrich) events in the North Atlantic: Geology, v. 20, p. 1087−1090.

BERTOK, C., MARTIRE, L., PEROTTI, E., D'ATRI, A., AND PIANA, F., 2011, Middle-Late Jurassic syndepositional tectonics recorded in the Ligurian Briançonnais succession (Marguareis–Mongioie area, Ligurian Alps, NW Italy): Swiss Journal of Geosciences, v. 104, p. 237–255.

Bertok, C., Martire, L., Perotti, E., d'Atri, A., and Piana, F., 2012, Kilometre-scale palaeoescarpments as evidence for Cretaceous synsedimentary tectonics in the External Briançonnais Domain (Ligurian Alps, Italy): Sedimentary Geology, v. 251-252, p. 58–75.

Bigi, G., Cosentino, D., Parotto, M., Sartori, R., and Scandone, P., 1990, Structural Model of Italy 1:500000, sheet 1: Firenze, SELCA.

Bone, Y., James, N.P., and Kyser, T.K., 1992, Synsedimentary detrital dolomite in Quaternary cool-water carbonate sediments, Lacepede shelf, South Australia, Geology, v. 20, p. 109−112.

Cander, H.S., Kaufman, J., Daniels, L.D., and Meyers, W.J., 1988, Regional dolomitization of shelf carbonates in the Burlington-Keokuk Formation (Mississippian), Illinois and Missouri: constraints from cathodoluminescent zonal stratigraphy, *in* Shukla, V., and Baker, P.A., eds., Sedimentology and Geochemistry of Dolostones: SEPM, Special Publication 43, p. 129−144.

Choquette, P.W., and Hiatt, E.E., 2008, Shallow-burial dolomite cement: a major component of many ancient sucrosic dolomites: Sedimentology, v. 55, p. 423−460.

Coniglio, M., and James, N.P:, 1988, Dolomitization of deep-water sediments, Cow Head Group (Cambro-Ordovician), western Newfoundland, Journal of Sedimentary Petrology, v. 58, p. 1032−1045.

Cullen, H.M., deMenocal, P.B., Hemming, S., Hemming, G., Brown, F.H., Guilderson, T., and Sirocko, F., 2000, Climate change and the collapse of the Akkadian empire: evidence from the deep sea: Geology, v. 28, p. 379−382.

Decarlis, A., and Lualdi, A., 2008, Late Triassic-Early Jurassic paleokarst from the Ligurian Alps and its geological significance (Siderolitico Auct., Ligurian Briançonnais domain): Swiss Journal of Geosciences, v. 101, p. 579–593.

Ehrenberg, S.N., McArthur, J.M., and Thirlwall, M.F., 2006, Growth, demise, and dolomitization of Miocene carbonate platforms on the Marion Plateau, offshore NE Australia: Journal of Sedimentary Research, v. 76, p. 91−116.

Evamy, B.D., and Shearman, D.J., 1965, The development of overgrowths from echinoderm fragments: Sedimentology, v. 5, p. 211−233.

Faure, J. L., and Megard-Galli, J., 1988, L'émersion jurassique en Briançonnais: sédimentation continentale et fracturation distensive: Société Géologique de France, Bulletin, v. 4, p. 681–692.

Freeman, T., Rothbard, D., and Obrador, A., 1983, Terrigenous dolomite in the Miocene of Menorca (Spain): provenance and diagenesis, Journal of Sedimentary Petrology, v. 53, p. 543−548.

Gandolfi, G., Paganelli, L., and Zuffa, G.G., 1983, Petrology and dispersal pattern in the Marnoso-Arenacea Formation (Miocene, Northern Apennines), Journal of Sedimentary Petrology, v. 53, p. 493−507.

Gregg, J.M., and Shelton, K.L, 1990, Dolomitization and dolomite neomorphism in the back reef facies of the Bonneterre and Davis Formations (Cambrian), southeastern Missouri. Journal of Sedimentary Petrology, v. 60, p. 549−562.

Gregg, J.M., Laudon, P.R., Woody, R.E., and Shelton, K.L., 1993, Porosity evolution of the Cambrian Bonneterre Dolomite, south-eastern Missouri, USA: Sedimentology, v. 40, p. 1153−1169.

Hardie, L.A., 1987, Dolomitization: a critical view of some current views: Journal of Sedimentary Petrology, v. 57, p. 166−183.

Harris, D.C., and Meyers, W.J., 1987, Regional dolomitization of subidal shelf carbonates: Burlington and Keokuk Formations (Mississippian), Iowa and Illinois, *in* Marshall, J.D., ed., Diagenesis of Sedimentary Sequences: Geological Society of London, Special Publication 36, p. 237−258.

James, N.P., and Bone, Y., 2007, A Late Pliocene–Early Pleistocene, inner-shelf, subtropical, seagrass-dominated carbonate: Roe Calcarenite, Great Australian Bight, Western Australia: Palaios, v. 22, p. 343−359.

JI, J., GE, Y., BALSAM, W., DAMUTH, J.E., AND CHEN, J., 2009, Rapid identification of dolomite using a Fourier Transform Infrared Spectrophotometer (FTIR): a fast method for identifying Heinrich events in IODP Site U1308: Marine Geology, v. 258, p. 60−68.

JONES, B., 2005, Dolomite crystal architecture: genetic implications for the origin of the Tertiary dolostones of the Cayman Islands: Journal of Sedimentary Research, v. 75, p. 177−189.

JONES, B., 2007, Inside-out dolomite: Journal of Sedimentary Research, v. 77, p. 539−551.

JONES, B., AND LUTH, R.W., 2002, Dolostones from Grand Cayman, Bristish West Indies: Journal of Sedimentary Research, v. 72, p. 560−570.

KNIES, J., VOGT, C., AND STEIN, R., 1999, Late Quaternary growth and decay of the Svalbard/Barents Sea ice sheet and paleoceanographic evolution in the adjacent Arctic Ocean: Geo-Marine Letters, v. 18, p. 195−202.

LANTEAUME, M., RADULESCU, N., GRAVOS, M., FERAUD, J., 1990, Notice explicative, Carte Géologique de France (1/50.000), feuille Viève-Tende (948): Orléans, Bureau de Recherches Géologiques et Minières, 139 p.

LEMOINE, M., BAS, T., ARNAUD-VANNEAU, A., ARNAUD, H., DUMONT, T., GIDON, M., BOURBON, M., DEGRACIANSKY, P.C., RUDKIEWICZ, J.L., MEGARD-GALLI, J., AND TRICART, P., 1986, The continental margin of the Mesozoic Tethys in the Western Alps: Marine and Petroleum Geology, v. 3, p. 179–199.

LEMOINE, M., AND TRÜMPY, R., 1987, Pre-oceanic rifting in the Alps: Tectonophysics, v. 133, p. 305–320.

LINDHOLM, R.C., 1969, Detrital dolomite in Onondaga limestone (Middle Devonian) of New York: its implications to the “Dolomite question”: American Association of Petroleum Geologists, Bulletin, v. 53, p. 1035−1042.

LYDAY, J.R., 1985, Atokan (Pennsylvanian) Berlin Field: genesis of recycled detrital dolomite reservoir, deep Anadarko Basin, Oklahoma: American Association of Petroleum Geologists, Bulletin, v. 69, p. 1931−1949.

Machel, H.G., 1997, Recrystallization versus neomorphism, and the concept of significant recrystallization in dolomite research: Sedimentary Geology, v. 113, p. 161−168.

Machel, H.G., 2000, Applications of cathodoluminescence to carbonate diagenesis, *in* Pagel, M., Barbin, V., Blanc, P., and Ohnenstetter, D., eds., Cathodoluminescence in geosciences: New York, Springer, p. 271−301.

Machel, H.G., 2004, Concepts and models of dolomitization: a critical reappraisal, *in* Braithwaite, C.J.R., Rizzi, G., and Darke, G., eds., The Geometry and Petrogenesis of Dolomite Hydrocarbon Reservoirs: Geological Society of London, Special Publication 235, p. 7−63.

Machel, H.G., and Burton, E.A., 1991, Factors governing cathodoluminescence in calcite and dolomite and their implications for studies of carbonate diagenesis, *in* Barker, C.E., and KOPP, O.C., eds., Luminescence Microscopy and Spectroscopy: Qualitative and Quantitative Applications: SEPM, Short Course 25, p. 37−57.

Meister, P., McKenzie, J.A., Bernasconi, S.M., and Brack, P., 2013, Dolomite formation in the shallow seas of the Alpine Triassic: Sedimentology, v. 60, p. 270−291.

Mohn, G., Manatschal, G., Müntener, O., Beltrando, M., and Masini, E., 2010, Unravelling the interaction between tectonic and sedimentary processes during lithospheric thinning in the Alpine Tethys margins: International Journal of Earth Sciences, v. 99, p. 75−101.

Morrow, D.W., Cumming, G.L., and Koepnick, R.B., 1986, Manetoe facies – a gas-bearing, megacrystalline, Devonian dolomite, Yukon and Northwest territories, Canada: American Association of Petroleum Geologists, Bulletin, v. 70, p. 702−720.

Murray, R.C., 1964, The origin of porosity in carbonate rocks, *in* Imbrie, J., and Newell, N., eds., Approaches to Palaeoecology: New York, John Wiley, p. 388−403.

Mussman, W.J, and Read, J.F., 1986, Sedimentology and development of a passive- to convergent-margin unconformity: Middle Ordovician Knox unconformity, Virginia Appalachians, Geological Society of America, Bulletin, v. 97, p. 282−295.

Piana, F., Musso, A., Bertok, C., d'Atri, A., Martire, L., Perotti, E., Varrone, D., and Martinotti, G., 2009, New data on post-Eocene tectonic evolution of the External Ligurian Briançonnais (Western Ligurian Alps): Italian Journal of Geosciences, v. 128, p. 353−366.

Pouchou, J.L., and Pichoir, F., 1988, Determination of mass absorption coefficients for soft X-rays by use of the electron microprobe, *in* Newbury, D.E., ed., Microbeam Analysis: San Francisco: San Francisco Press, p. 319−324.

Reeder, R.J., 1991, An overview of zoning in carbonate minerals, *in* Barker, C.E., and Kopp, O.C., eds., Luminescence Microscopy and Spectroscopy: Qualitative and Quantitative Applications: SEPM, Short Course 25, p. 77−82.

Reinhold, C., 1998, Multiple episodes of dolomitization and dolomite recrystallization during shallow burial in Upper Jurassic shelf carbonates: eastern Swabian Alb, southern Germany: Sedimentary Geology, v. 121, p. 71−95.

Sibley, D.F., 1982, The origin of common dolomite fabrics: clues from the Pliocene: Journal of Sedimentary Petrology, v. 52, p. 1087−1100.

Taylor, K.G., Gawthorpe, R.L., Curtis, C.D., Marshall, J.D., and Awwiller, D.N., 2000, Carbonate cementation in a sequence-stratigraphic framework: Upper Cretaceous sandstones, Book Cliffs, Utah–Colorado: Journal of Sedimentary Research, v. 70, p. 360–372.

Taylor, K.G., Gawthorpe, R.L., and Fannon-Howell, S., 2004, Basin-scale diagenetic alteration of shoreface sandstones in the Upper Cretaceous Spring Canyon and Aberdeen Members, Blackhawk Formation, Book Cliffs, Utah: Sedimentary Geology, v. 172, p. 99−115.

Vanossi, M., 1965, Le unità stratigrafico-strutturali tra il Pizzo di Ormea e il Monte Galero (Alpi Marittime): Università di Pavia, Istituto Geologico, Atti, v. 16, p. 114−184.

Vanossi, M., Cortesogno, L., Galbiati, B., Messiga, B., Piccardo, G., and Vannucci, R., 1984, Geologia delle alpi liguri: dati, problemi, ipotesi: Società Geologica Italiana, Memorie, v. 28, p. 5–75.

WALKDEN, G.M., AND BERRY, J.R., 1984, Natural calcite in cathodoluminescence: crystal growth during diagenesis: Nature, v. 308, p. 525−527.

YOUNG, H.R., AND DOIG, D.J., 1986, Petrography and provenance of the glauconitic sandstone, South-Central Alberta, with comments on the occurrence of detrital dolomite: Bulletin of Canadian Petroleum Geology, v. 34, p. 408−425.

FIGURE CAPTIONS

Figure 1. Simplified geological map with the main tectonostratigraphic units and domains of the southwestern portion of the Alps. The black square indicates the study area. (Redrawn after Bigi et al., 1990).

Figure 2. Log of the stratigraphic succession of the study area. QPN Quarziti di Ponte di Nava (quartzarenite); PCV Peliti di Case Valmarenca (mudrock); DSPM Dolomie di S. Pietro dei Monti (dolostone and dolomitic limestone); CRN Calcari di Rio di Nava (limestone and dolomitic limestone); CVT Calcari di Val Tanarello (pelagic limestone); FU Formazione di Upega (marly limestone); CMC Calcari della Madonna dei Cancelli (nummulite-rich limestone); FN Flysch Noir (interbedded mudrock and sandstone).

Figure 3. A) Transmitted-light photomicrograph and B) CL image showing the stratigraphic boundary between the Middle Triassic DSPM and the overlying the Middle Jurassic CRN. Note: the greenish luminescence of the very finely to finely crystalline DSPM dolostones (compare with Figure 11); the coarser size of the subhedral to euhedral dolomite crystals in the CRN, composed of irregular cores with different luminescences (NL, dull red) surrounded by a thin bright orange rim; the occurrence of dull blue luminescing quartz grains.

Figure 4. Transmitted-light photomicrograph showing a grainstone as the matrix of the transgressive conglomerate locally occurring at the base of the Middle Jurassic CRN and including

lithoclasts of Middle Triassic DSPM: note a dolomite crystal with a pitted edge at the core of a coated grain.

Figure 5: Clast- to matrix-supported breccia bed with angular to rounded clasts made of light Middle Triassic DSPM interbedded with micritic limestone in the lower part of the Middle Jurassic CRN. Tip of pencil at the bottom for scale is 7 cm long.

Figure 6. A) Transmitted-light photomicrograph of a partly dolomitized Middle Jurassic CRN micritic limestone. The white square indicates the CL close up of Fig. 6B. B) CL image of the squared area in Part A. Note: the commonly euhedral habit of dolomite crystals; the internal zoning; the irregular shape of the nonluminescent cores. For further details see text.

Figure 7. A) Transmitted light photomicrograph and B) CL image of a partly dolomitized Middle Jurassic CRN micritic limestone. Note in the CL image the differently luminescing cores of dolomite crystals, ranging from NL to dull red to greenish.

Figure 8. A) Transmitted light photomicrograph and B) CL image of a partly dolomitized Middle Jurassic CRN micritic limestone. Note in the CL image the differently luminescing cores of dolomite crystals, ranging from NL to moderate red.

Figure 9. Sketch summarizing the main features of the different zones of dolomite rhombs. Ca:Mg ratios are average values. Among the three possibilities of CL colors of the cores (NL, red and greenish), the green one has been chosen not to make confusion with the red or NL color of rim zones.

Figure 10. BSE image of a partly dolomitized Middle Jurassic CRN limestone. Note: the contrast between the homogeneous core and the outer rims spotted with brighter micrometer-size calcite; the lighter color of rims compared to that of the core, related to higher amounts of Ca in dolomite.

Figure 11. A) Transmitted-light photomicrograph and B) CL image of a partly dolomitized Middle Jurassic CRN micritic limestone. The CL image shows the greenish luminescence of a finely crystalline lithoclast of Middle Triassic DSPM (compare with Fig. 3).

Figure 12. A) Transmitted-light photomicrograph, B) CL image, and C) BSE image of a dolomite-filled vein crosscutting the finely crystalline Middle Triassic DSPM dolostones. The white square in Part B indicates the BSE close-up of Part C. In the CL image, four growth zones (I to IV) of dolomite cement are clearly evidenced by NL, bright orange, moderate orange and NL luminescence. In the BSE image the higher Fe content of zones I and IV is evidenced by lighter colors.

Figure 13. Cartoon sketching the main phases (1 to 4) of formation of the dolomite. Detrital fragments of dolomite (in green) are deposited together with carbonate mud in Middle Jurassic limestone (1). A first generation of NL dolomite (in black) precipitates only as cement in fractures (2). The subsequent flow of fluids undersaturated in calcite and slightly supersaturated in dolomite results in formation of the same dolomite zones (in bright red, moderate red and dark grey) both in veins and as syntaxial overgrowths around detrital cores (3-4).

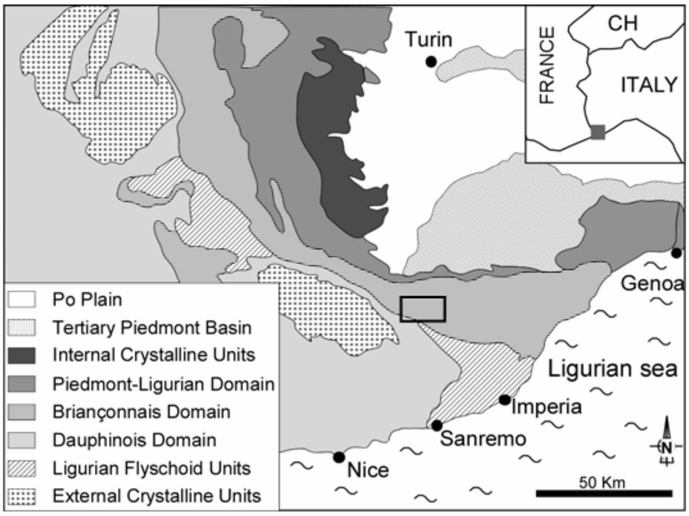
Turin
FRANCE
CH
ITALY
Genoa
Ligurian sea
Imperia
Sanremo
Nice
N
50 Km
Po Plain
Tertiary Piedmont Basin
Internal Crystalline Units
Piedmont-Ligurian Domain
Briançonnais Domain
Dauphinois Domain
Ligurian Flyschoid Units
External Crystalline Units

Fig. 1

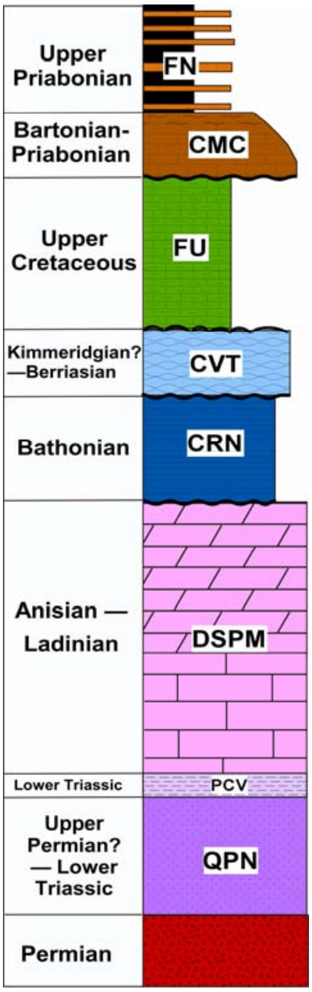
Upper Priabonian
FN
Bartonian-Priabonian
CMC
Upper Cretaceous
FU
Kimmeridgian?—Berriasian
CVT
Bathonian
CRN
Anisian — Ladinian
DSPM
Lower Triassic
PCV
Upper Permian? — Lower Triassic
QPN
Permian

Fig. 2

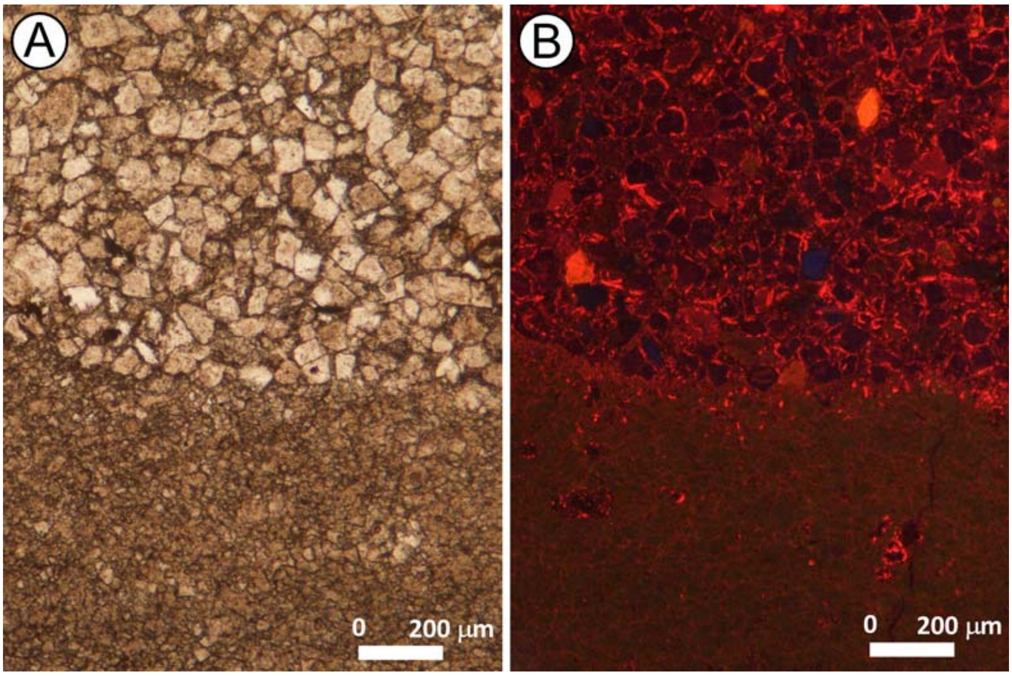

Fig. 3

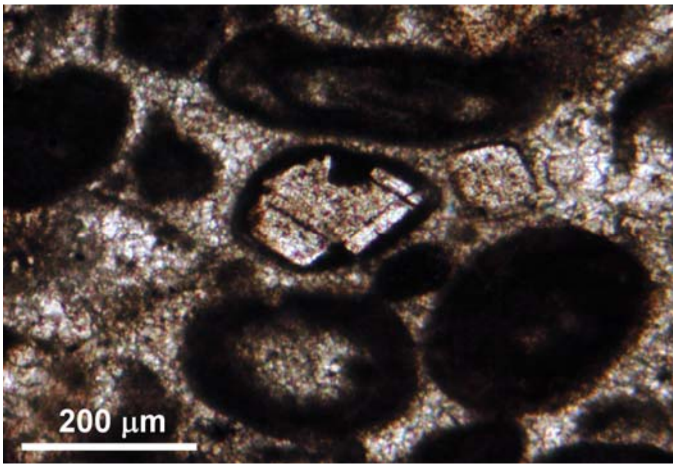

Fig. 4

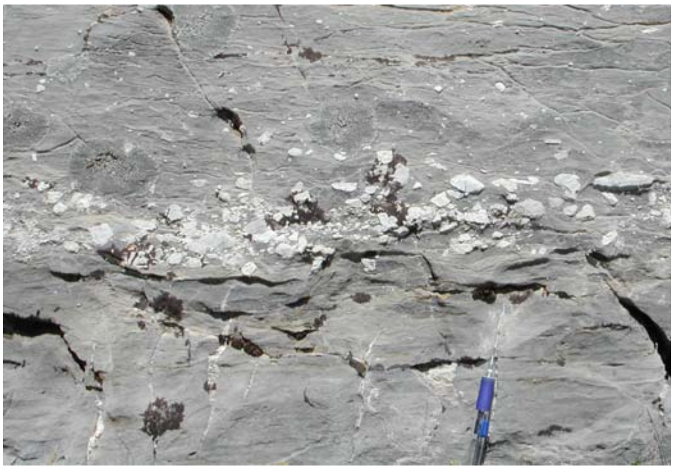

Fig. 5

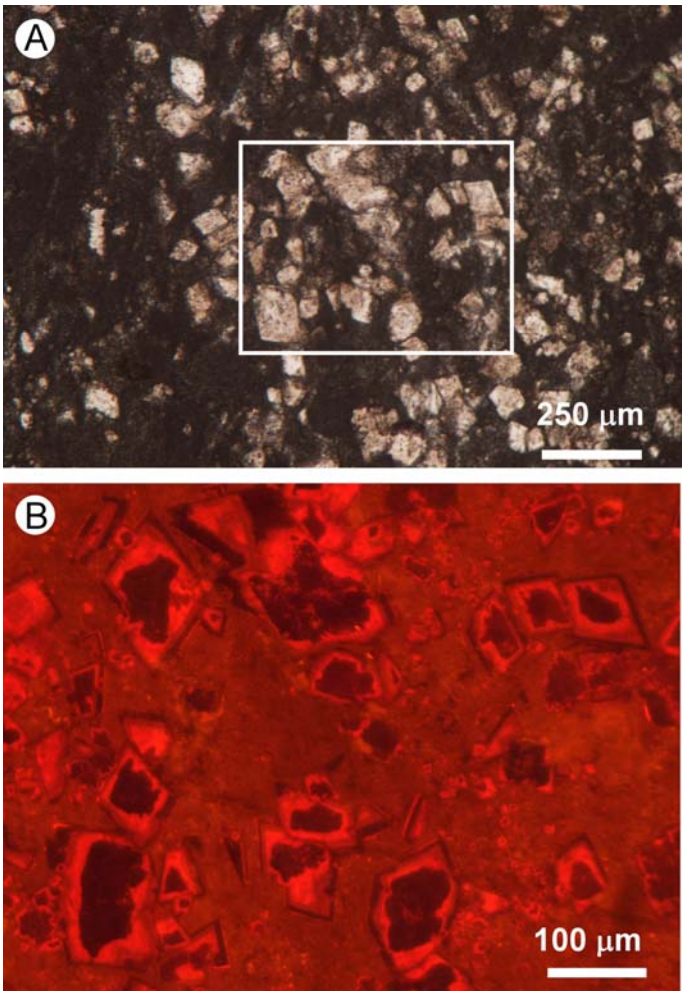

Fig. 6

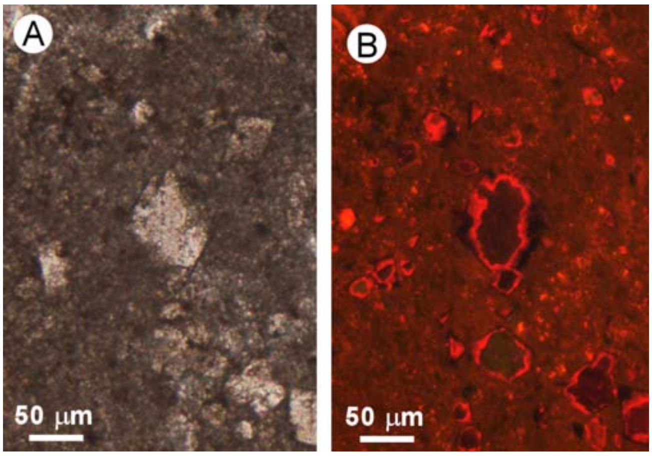

Fig. 7

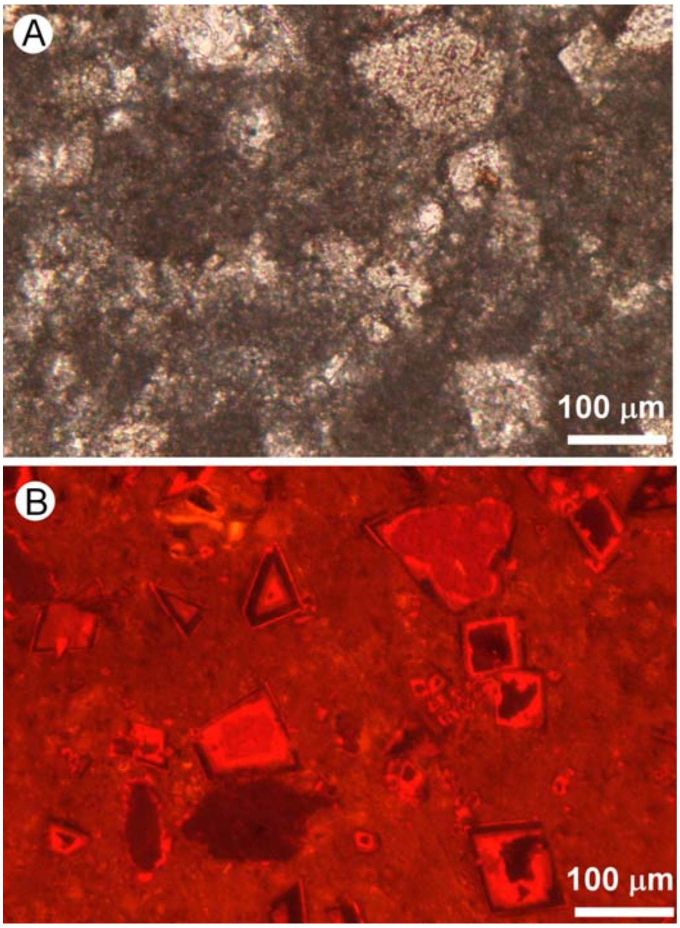

Fig. 8

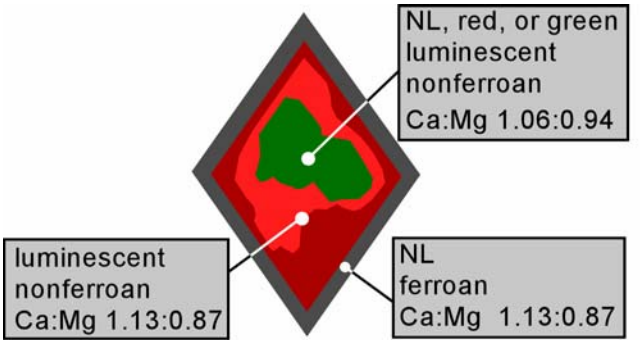

Fig. 9

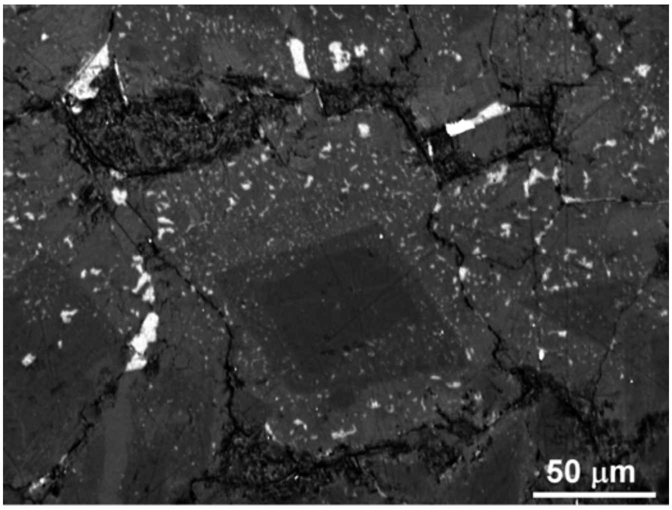

Fig. 10

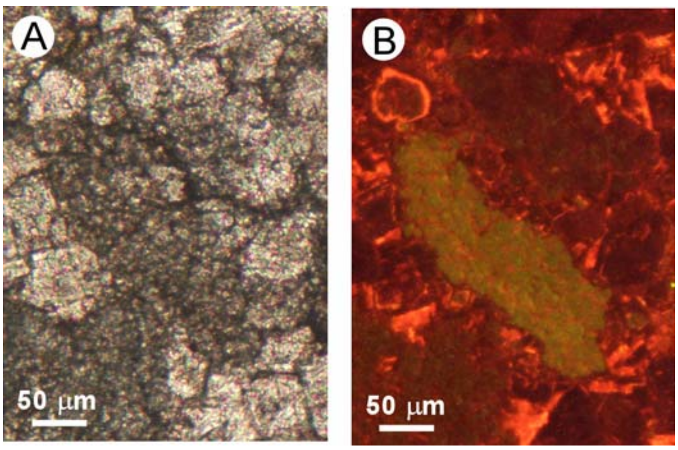

Fig. 11

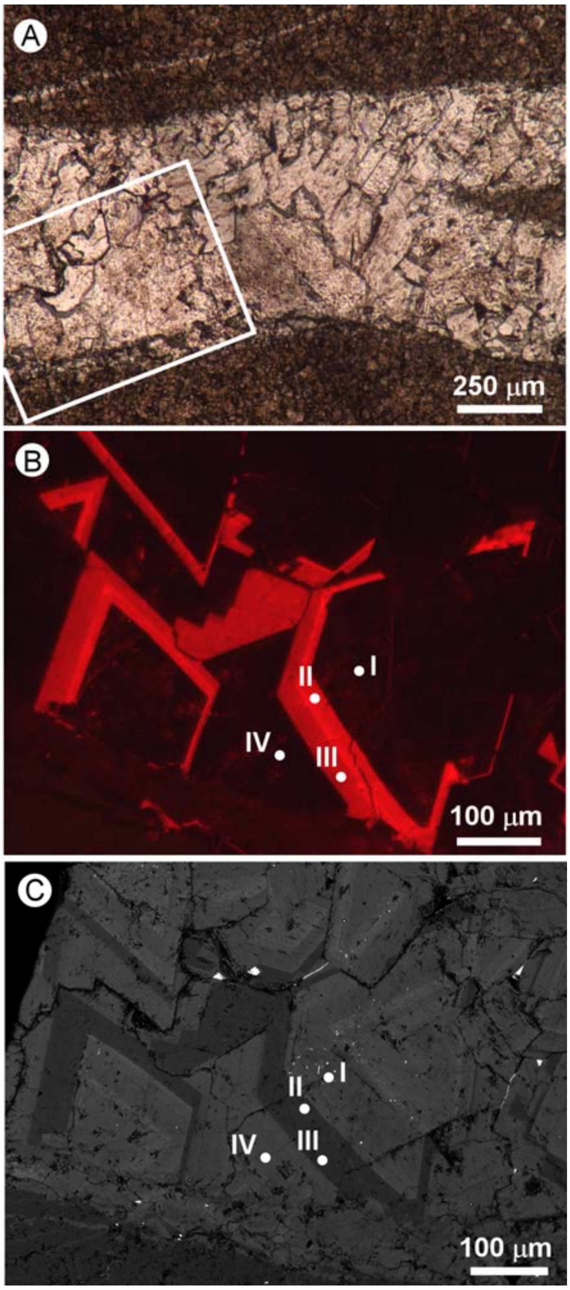

Fig. 12

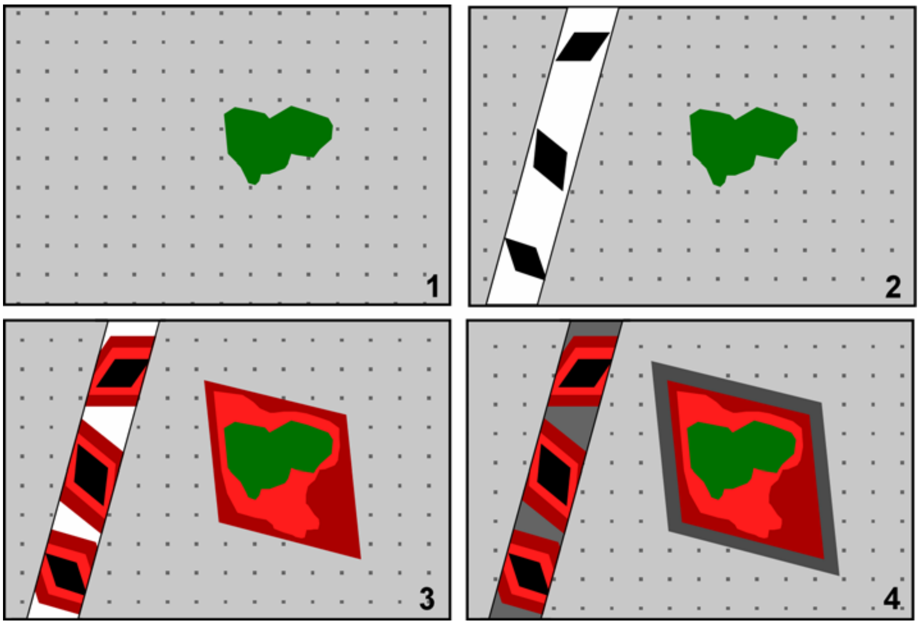

Fig. 13